Eight Lissajous orbits in the Earth-Moon system

Grégory Archambeau, Philippe Augros, Emmanuel Trélat

Noname manuscript No.
(will be inserted by the editor)

Eight Lissajous orbits in the Earth-Moon system

G. Archambeau · P. Augros · E. Trélat

Received: date / Accepted: date

Abstract Euler and Lagrange proved the existence of five equilibrium points in the circular restricted three-body problem. These equilibrium points are known as Lagrange points (Euler points or libration points) $L_1, \ldots, L_5$. The existence of families of periodic and quasi-periodic orbits around those points is well known (see [15,16,31]). Among them, halo orbits are 3-dimensional periodic orbits diffeomorphic to circles. They are the first type of so-called Lissajous orbits. In this article we focus on Lissajous orbits of the second type, which are almost vertical and have the shape of an eight, and that we call Eight Lissajous orbits. In the Earth-Moon system, we first compute numerically a family of such orbits, based on Linsdtedt Poincaré's method combined with a continuation method on the excursion parameter. Then, we study their specific properties. In particular, we put in evidence, using local Lyapunov exponents, that their invariant manifolds share nice global stability properties, which make them of interest in space mission design. More precisely, we show numerically that invariant manifolds of Eight Lissajous orbits keep in large time a structure of eight-shaped tubes. This property is compared with halo orbits, the invariant manifolds of which do not share such global stability properties. Finally, we show that the invariant manifolds of Eight Lissajous orbits can be used to visit almost all the Moon surface in the Earth-Moon system.

This work was granted by EADS les Mureaux, France.

G. Archambeau
Univ. Paris-Sud, Labo. Math., UMR 8628, Bat. 425, 91405 Orsay Cedex, France
E-mail: gregory.archambeau@math.u-psud.fr

P. Augros
EADS SPACE Transportation SAS, Flight Control Group, 66 route de Verneuil, BP 3002, 78133 Les Mureaux Cedex, France
Phone: +33 (0)1 39 06 12 64
Fax: +33 (0)1 39 06 19 99
E-mail: philippe.augros@space.eads.net

E. Trélat
Université d'Orléans, Laboratoire MAPMO, CNRS, UMR 6628, Fédération Denis Poisson, FR 2964, Bat. Math., BP 6759, 45067 Orléans cedex 2, France
Phone: +33 (0)2 38 49 47 25
Fax: +33 (0)2 38 41 72 05
E-mail: emmanuel.trelat@univ-orleans.fr

Keywords Lagrange points · Lissajous orbits · stability · mission design

PACS PACS 95.10.Ce · PACS 95.10.Eg

Mathematics Subject Classification (2000) MSC 70F07 · MSC 37N05

1 Introduction

In the restricted three-body problem, the existence of periodic orbits around the Lagrange points is very well known. Lyapunov orbits (planar orbits) are quite easy to compute and Richardson's work (see [31]) provides a third-order approximation of the classical halo orbits (3-dimensional orbits isomorphic to ellipses) which allows to compute families of halo orbits through a shooting method. Besides Lyapunov and halo orbits, there exist other types of periodic orbits around the Lagrange points, in particular Lissajous orbits (see[15–18, **?**]). Among those periodic orbits, we focus here on the Lissajous periodic orbits which can be considered as Lissajous orbits of the second kind, that we call Eight Lissajous orbits, and that are almost vertical and have the shape of an eight. In the first part of the article, we report on the circular restricted three-body problem and recall how to compute families of Eight Lissajous orbits using a Newton's method, that we combine with a continuation method on the excursion parameter. A third-order approximation of Eight Lissajous is calculated using Linstedt Poincaré's method, which serves as an initial guess. Then, stability properties of invariant manifolds of Eight Lissajous orbits are studied and compared to those of halo orbits. Using local Lyapunov exponents, we prove that invariant manifolds of Eight Lissajous orbits share strong global stability properties which make them of great interest in mission design analysis. Finally, to provide a relevant example of their applicability, we investigate the accessibility to the Moon surface exploration using Eight Lissajous manifolds.

1.1 Recalls on the circular restricted three-body problem

The circular restricted three-body problem concerns the movement of a body P in the gravitational field of two masses m_1 and m_2, where the mass of P is negligible with respect to m_1 and m_2. The masses m_1 and m_2 (with $m_1 \geq m_2$) are called the primaries and are assumed to have circular coplanar orbits with the same period around their center of mass. In this problem, the influence of any other body is neglected. If the body P is further restricted to move in the plane of the two primaries, the problem is then called planar circular restricted three-body problem.

In the solar system it happens that the circular restricted three-body problem provides a good approximation for studying a large clas of problems. In our application, the Earth-Moon system shall be considered. Thus, the primaries are the Earth and the Moon and gravitational forces exerted by any other planet or any other body are neglected.

In an inertial frame, the primaries positions and the equations of motion of P are time-dependent. It is thus standard to derive the equations of motion of P in a rotating frame whose rotation speed is equal to the rotation speed of the primaries around their center of mass, and whose origin is in the orbital plane of the masses m_1 and m_2. In such a frame, the positions of m_1 and m_2 are fixed. We consider the rotating frame

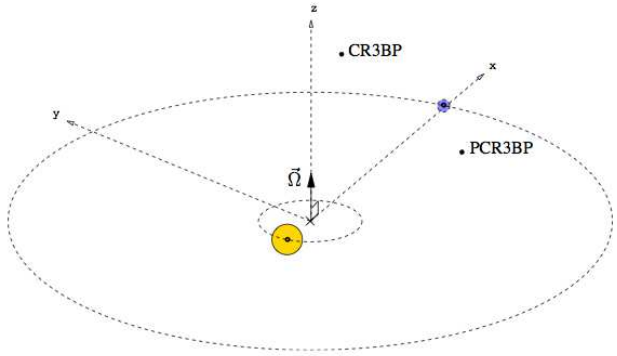

Fig. 1 The restricted three-body problem

with the x axis on the m_1-m_2 line and with origin at the libration point considered. The masses m_1 and m_2 move in the xy plane and the z axis is orthogonal to this plane. In addition, we adopt an adimensional unit system with the following agreements: the distance between the Lagrange point considered and the closer primary is 1; the sum of the masses m_1 and m_2 is 1; the angular velocity of the primaries is 1. The body is submitted to the gravitational attraction forces exerted by the primaries, the Coriolis force and the centrifugal force. Denote by

$$X = (x, y, z, \dot{x}, \dot{y}, \dot{z})^T = (x_1, x_2, x_3, x_4, x_5, x_6)^T$$

the position and velocity vector of P in the rotating frame. The equations of motion are

$$\begin{aligned} \ddot{x} - 2\dot{y} &= \frac{\partial \Phi}{\partial x} \\ \ddot{y} + 2\dot{x} &= \frac{\partial \Phi}{\partial y} \\ \ddot{z} &= \frac{\partial \Phi}{\partial z} \end{aligned} \tag{1}$$

where

$$\Phi(x, y, z) = \frac{x^2 + y^2}{2} + \frac{1-\mu}{r_1} + \frac{\mu}{r_2} + \frac{\mu(1-\mu)}{2},$$

and

$$r_1 = \sqrt{(x+\mu)^2 + y^2 + z^2}, \quad r_2 = \sqrt{(x-1+\mu)^2 + y^2 + z^2},$$

and where $x = x_1$ and $y = x_2$ are the abscisses of the primaries m_1 and m_2. Recall that these equations admit a trivial first integral, called Jacobi integral,

$$J = x^2 + y^2 + 2\frac{1-\mu}{r_1} + 2\frac{\mu}{r_2} + \mu(1-\mu)) - (\dot{x}^2 + \dot{y}^2 + \dot{z}^2),$$

related to the energy. Hence, if an energy level is fixed, the solutions live in a 5-dimensional energy manifold. The study of that manifold determines the so-called Hill's region of possible motion (see e.g. [19]).

The Lagrange points are the equilibrium points of the circular restricted three-body problem. Euler [10] and Lagrange [20] proved the existence of five equilibrium points, three collinear points on the axis joining the center of the two primaries, generally noted L_1, L_2 and L_3, and two equilateral points noted L_4 and L_5 (see Figure 2).

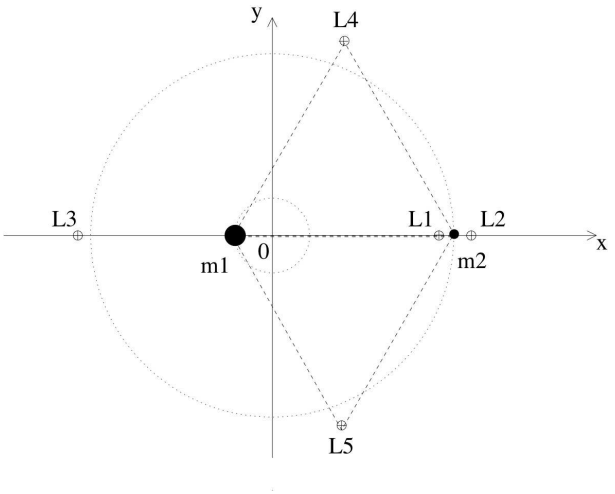

Fig. 2 Lagrange points

For a precise computation of the coordinates of Lagrange points, we refer the reader to [34] (see also [19]). Concerning their stability, we recall that the collinear points are shown to be unstable in every system, whereas L_4 and L_5 are proved to be stable under some conditions (see [26]). Actually, it follows from a generalization of a theorem of Lyapunov, due to Moser (see [28]), that, for a value of the Jacobi integral a bit less than that of Lagrange points, the solutions of the nonlinear system have the same qualitative behavior than the solutions of the linearized system, in the vicinity of Lagrange points.

Let us focus on the three collinear Lagrange points. It is standard to expand the nonlinear terms $\frac{1}{r_1}$ and $\frac{1}{r_2}$ as series with Legendre polynomials, using the formula

$$\frac{1}{\sqrt{(x-A)^2+(y-B)^2+(z-C)^2}} = \frac{1}{D}\sum_{n=0}^{+\infty}\left(\frac{\rho}{D}\right)^n P_n\left(\frac{Ax+By+Cz}{D\rho}\right),$$

where $D^2 = A^2+B^2+C^2+D^2$ and $\rho = x^2+y^2+z^2$, and this leads to write the equations of motion (1) around the libration point L_i, $i = 1, 2, 3$, as

$$\begin{aligned}
\ddot{x} - 2\dot{y} - (1+2c_2)x &= \frac{\partial}{\partial x}\sum_{n\geq 3} c_n\rho^n P_n\left(\frac{x}{\rho}\right),\\
\ddot{y} + 2\dot{x} + (c_2-1)x &= \frac{\partial}{\partial y}\sum_{n\geq 3} c_n\rho^n P_n\left(\frac{x}{\rho}\right),\\
\ddot{z} + c_2 z &= \frac{\partial}{\partial z}\sum_{n\geq 3} c_n\rho^n P_n\left(\frac{x}{\rho}\right),
\end{aligned} \tag{2}$$

where

$$c_n = \frac{1}{\gamma_i^{(n+1)}} \left(\mu + \frac{(1-\mu)\gamma_i^{(n+1)}}{(1-\gamma_i)^{(n+1)}} \right).$$

Here, γ_i denotes the distance between the Lagrange point L_i and the second primary.

At the Lagrange points L_1, L_2, L_3, the linearized system consists of the linear part of equations (2),

$$\begin{aligned} \ddot{x} - 2\dot{y} - (1 + 2c_2)x = 0, \\ \ddot{y} + 2\dot{x} + (c_2 - 1)x = 0, \\ \ddot{z} + c_2 z = 0. \end{aligned}$$

It is of the type saddle×center×center, with eigenvalues $(\pm\lambda, \pm i\omega_p, \pm i\omega_v)$, where

$$\lambda^2 = \frac{c_2 - 2 + \sqrt{9c_2^2 - 8c_2}}{2}, \quad \omega_p^2 = \frac{2 - c_2 + \sqrt{9c_2^2 - 8c_2}}{2}, \quad \omega_v^2 = c_2.$$

Lyapunov-Poincaré's Theorem implies the existence of a two-parameter family of periodic trajectories around each point (see [26], or see for instance [6]). One can also see this two-parameter family as two one-parameter families of periodic orbits. Halo orbits are periodic orbits around Lagrange points, which are diffeomorphic to circles. Their interest for mission design was first pointed out by Farquhar (see [11,12]. Other families of periodic orbits, called Lissajous orbits, have been put in evidence and computed in [15], so as quasi-periodic orbits (see [16]). Halo orbits may be seen as Lissajous orbits of the first kind, and in the present article we are interested in Lissajous orbits of the second kind, topologically equivalent to eight-shaped curves. Their existence and the way to compute them is recalled in Section 2.

Given a periodic orbit around a Lagrange point, the stable (resp., unstable) manifold of this orbit is defined as the submanifold of the phase space which is formed by all points whose future (resp., past) semi-orbits converge to the periodic orbit (such orbits are said asymptotic). It is well known that invariant manifolds of Lissajous orbits act as separatrices, in the following sense (see [14]). Invariant manifolds are kinds of 4-dimensional tubes, topologically equivalent to $S^3 \times \mathbb{R}$, in the 5-dimensional energy manifold mentioned formerly. Due to this dimensionality, it happens that they separate two types of orbits, called transit orbits and non-transit orbits. The transit orbits are defined as orbits passing from one region to another, inside the 4-dimensional tubes. The non-transit orbits are outside the tubes.

2 Eight Lissajous orbits

2.1 Periodic solutions of the linearized equations

Let us first investigate the solutions of the linearized system (2) around L_i, $i = 1, 2, 3$. If the initial conditions are restricted to the non divergent modes, the bounded solutions of the linear system are written as

$$\begin{aligned} x(t) &= -A_x cos(\omega_p t + \phi), \\ y(t) &= \kappa A_y sin(\omega_p t + \phi), \\ z(t) &= A_z cos(\omega_v t + \psi), \end{aligned} \tag{3}$$

where

$$\kappa = \frac{w_p^2 + 1 + c_2}{2\omega_p} = \frac{2\lambda}{\lambda^2 + 1 - c_2},$$

and A_x, A_y and A_z are generally refered to as the x-excursion, y-excursion and z-excursion. One can immediately observe that the bounded solutions of the linear system are periodic if the in-plane and the out-of-plane frequencies, ω_p and ω_v, have a rational ratio.

Moser's theorem mentioned formerly implies that bounded trajectories can also be found for the nonlinear system. They may be seen as perturbations of the bounded trajectories of the linear system, the nonlinear terms acting on the amplitudes and the frequencies. This change of frequencies induced by the nonlinearities has been used by Richardson to calculate an approximation of halo orbits (see [31]). We will use it in the next section to calculate an approximation of Eight Lissajous orbits.

In the expression of the bounded solutions of the linear system, the values of the frequencies ω_p and ω_v are naturally fixed by the system and the libration point considered. But, as explained before, these eigenfrequencies change for the nonlinear system. If the nonlinearities generate equal frequencies $\omega_p = \omega_v$, then halo orbits are obtained. This is what Richardson did to calculate an approximation of halo orbits. Similarly, if the quotient of the two eigenfrequencies is rational but different of the unity, other types of bounded solutions can be obtained (see [15,16]).

2.2 Lindstedt Poincaré's method

To calculate approximations of periodic solutions around the libration points, we use Lindstedt-Poincaré's method, based on the vision that the nonlinearities change the solutions of the linearized system by changing their eigenfrequencies. Since we aim at computing an Eight Lissajous orbit, we consider as a reference an eight-shaped orbit, with frequencies ω_p and ω_v satisfying $\omega_v = \frac{\omega_p}{2}$. With such values, the linearized equations are

$$\begin{aligned} &\ddot{x} - 2\dot{y} - (1 + 2c_2)x = 0, \\ &\ddot{y} + 2\dot{x} + (c_2 - 1)y = 0, \\ &\ddot{z} + \left(\tfrac{\omega_p}{2}\right)^2 z = 0, \end{aligned} \tag{4}$$

and admit periodic orbits parametrized by

$$\begin{aligned} x(t) &= -A_x \cos(\omega_p t + \phi), \\ y(t) &= \kappa A_y \sin(\omega_p t + \phi), \\ z(t) &= A_z \cos(\tfrac{\omega_p}{2} t + \psi), \end{aligned} \tag{5}$$

which are eight-shaped, diffeomorphic to the solution drawn on Figure (3).

Enforcing the relation $\omega_v = \frac{\omega_p}{2}$ in the equations of motion (2) leads to

$$\begin{aligned} \ddot{x} - 2\dot{y} - (1 + 2c_2)x &= \frac{\partial}{\partial x} \sum_{n \geq 3} c_n \rho^n P_n \left(\frac{x}{\rho}\right), \\ \ddot{y} + 2\dot{x} + (c_2 - 1)y &= \frac{\partial}{\partial y} \sum_{n \geq 3} c_n \rho^n P_n \left(\frac{x}{\rho}\right), \\ \ddot{z} + \left(\frac{\omega_p}{2}\right)^2 z &= \frac{\partial}{\partial z} \sum_{n \geq 3} c_n \rho^n P_n \left(\frac{x}{\rho}\right) + \Delta z, \end{aligned} \tag{6}$$

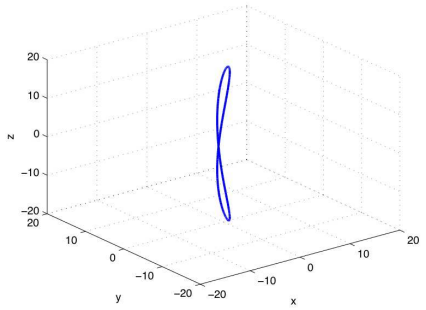

Fig. 3 Representation of the curve $x(t) = \cos(2t)$, $y(t) = \sin(2t)$, $z(t) = 20\cos(t)$, where $t \in [0, 2\pi]$.

where $\Delta = (\frac{\omega_p}{2})^2 - \omega_v^2$. In such a way, the reference orbit of the Linsdtedt-Poincaré's method is enforced to an eight-shaped orbit. Then, to take into account the fact that the nonlinearities affect the eigenfrequencies, the Linsdtedt-Poincaré's method consists in considering time-varying frequencies in the following way. Define

$$\tau = \nu t,$$

and the correction frequency

$$\nu = 1 + \sum_{n \geq 1} \nu_n, \ \nu_n < 1\cdot$$

The method consists then in adjusting iteratively the parameters ν_n so as to filter out secular terms which appear in the development of the successive approximations of the solution and are causing a blow up of the solutions. Let us introduce several notations and assumptions.

First, for every integer p and all elements v and w of $\mathbb{R}^p$, of coordinates in the canonical basis of $\mathbb{R}^p$,

$$v = \begin{pmatrix} v_1 \\ v_2 \\ \vdots \\ v_p \end{pmatrix} \quad \text{and} \quad w = \begin{pmatrix} w_1 \\ w_2 \\ \vdots \\ w_p \end{pmatrix},$$

define $v \cdot *w \in \mathbb{R}^p$ as the vector

$$v \cdot *w = \begin{pmatrix} v_1 w_1 \\ v_2 w_2 \\ \vdots \\ v_p w_p \end{pmatrix}.$$

With this notation, the reference solution writes

$$q_{ref}(\tau) = \begin{pmatrix} A_x \\ A_x \\ A_z \end{pmatrix} \cdot * \begin{pmatrix} -\cos(\omega_p \tau + \phi) \\ \kappa \sin(\omega_p \tau + \phi) \\ \sin(\frac{\omega_p}{2}\tau + \psi) \end{pmatrix} = \bar{A} \cdot * q_0(\tau).$$

The reference solution being considered as the first term of a series expansion, it is natural to seek a periodic solution in the form of a series in $\bar{A}$,

$$q(\tau) = \begin{pmatrix} x(\tau) \\ y(\tau) \\ z(\tau) \end{pmatrix} = \bar{A}\cdot * q_0 + \bar{A}^2 \cdot * q_1 + \bar{A}^3 \cdot * q_2 + \ldots = \begin{pmatrix} Ax_0(\tau) + A^2 x_1(\tau) + A^3 x_2(\tau) + \ldots \\ Ay_0(\tau) + A^2 y_1(\tau) + A^3 y_2(\tau) + \ldots \\ Az_0(\tau) + A^2 z_1(\tau) + A^3 z_2(\tau) + \ldots \end{pmatrix} \tag{7}$$

where A^n stands for the two-variables polynomial of degree n

$$A^n = \sum_{\substack{l,p=1 \\ l+p=n}}^{n} \lambda_{l,p} A_x^l A_z^p.$$

Note that considering an n-th-order approximation of the solution amounts to truncating the series expansion at order n. Finally, the ν_n are assumed to have the same order than A^n. We next rewrite the equations of motion in terms of these variables,

$$\begin{aligned} \nu^2\ddot{x} - 2\nu\dot{y} - (1+2c_2)x &= \frac{3}{2}(2x^2 - y^2 - z^2) + 2c_4 x(2x^2 - 3y^2 - 3z^2) + 0(4), \\ \nu^2\ddot{y} + 2\nu\dot{x} + (c_2 - 1)y &= -3c_3 xz - \frac{3}{2}c_4 y(4x^2 - y^2 - z^2) + 0(4), \\ \nu^2\ddot{z} + (\frac{\omega_p}{2})^2 z &= -3c_3 xz - \frac{3}{2}c_4 z(4x^2 - y^2 - z^2) + \Delta z + 0(4), \end{aligned} \tag{8}$$

where $O(4)$ denotes terms of order greater than or equal to 4. Then, plugging the series expansion (7) into (8), one gets:

– at the first order in A:

$$\begin{aligned} A_x\ddot{x}_0 - 2A_x\dot{y}_0 - (1+2c_2)A_x x_0 &= 0, \\ A_x\ddot{y}_0 + 2A_x\dot{x}_0 + (c_2 - 1)A_x y_0 &= 0, \\ A_z\ddot{z}_0 + A_z(\frac{\omega_p}{2})^2 z_0 &= 0; \end{aligned}$$

– at the second order in A:

$$\begin{aligned} A^2\ddot{x}_1 - 2A^2\dot{y}_1 - (1+2c_2)A^2 x_1 &= -2\nu_1 A_x\ddot{x}_0 + 2\nu_1 A_x\dot{y}_0 \\ &\quad + \frac{3}{2}\left(2A_x^2 x_0^2 - A_x^2 y_0^2 - A_z^2 z_0^2\right), \\ A^2\ddot{y}_1 + 2A^2\dot{x}_1 + (c_2 - 1)A^2 y_1 &= -2\nu_1 A_x\ddot{y}_0 - 2\nu_1 A_x\dot{x}_0 - 3c_3 A_x^2 x_0 y_0, \\ A^2\ddot{z}_1 + (\frac{\omega_p}{2})^2 A^2 z_1 &= -2\nu_1 A_z\ddot{z}_0 - 3c_3 A_x A_z x_0 z_0; \end{aligned}$$

– at the third order in A:

$$\begin{aligned} A^3\ddot{x}_2 - 2A^3\dot{y}_2 - (1+2c_2)A^3 x_2 &= -2\nu_1 A^2\ddot{x}_1 - (\nu_1 + 2\nu_2)A_x\ddot{x}_0 + 2\nu_1 A^2\dot{y}_1 \\ &\quad + 2A^3\dot{y}_2 + 2\nu_2 A_x\dot{y}_0, \\ A^3\ddot{y}_2 + 2A^3\dot{x}_2 + (c_2 - 1)A^3 y_2 &= -2\nu_1 A^2\ddot{y}_1 - 2\nu_1 A^2\dot{x}_1 - (\nu_1^2 + 2\nu_2)A_x\ddot{y}_2 \\ &\quad - 2\nu_2 A_x\dot{x}_0 - 3c_3(A_x A^2 x_0 y_1 + A_x A^2 y_0 x_1) \\ &\quad - \frac{3}{2}c_4 A_x y_0(4A_x^2 x_0^2 - A_x^2 y_0^2 - A_z^2 z_0^2), \\ A^3\ddot{z}_2 + (\frac{\omega_p}{2})^2 A^3 z_2 &= -2\nu_1 A^2\ddot{z}_1 - (\nu_1^2 + 2\nu_2)A_z\ddot{z}_0 \\ &\quad - 3c_3(A_x A^2 x_0 z_1 + A_z A^2 x_1 z_0) + \Delta A_z z_0. \end{aligned}$$

Now, Lindstedt-Poincaré's method consists in adjusting the coefficients ν_n in function of A_x and A_z to filter out the secular terms that can appear in the expansion of the solution. Note that the presence of secular terms causes divergence of the series expansion and blow-up of the truncated solution.

At the first order in A, we recover the expected solution

$$\begin{pmatrix} x_0(\tau) \\ y_0(\tau) \\ z_0(\tau) \end{pmatrix} = \begin{pmatrix} -\cos(\omega_p\tau + \phi) \\ \kappa \sin(\omega_p\tau + \phi) \\ \sin(\frac{\omega_p}{2}\tau + \psi) \end{pmatrix}.$$

At the second order in A, equations in the (x, y)-plane are decoupled from the z-equation, and it is possible to choose ν_1 so as to filter out the possible secular terms which appear whenever modes of the second member of the differential equation coincide with modes of the first member. In our case, the modes of the equation without second member remain the same, that is $(\pm\lambda, \pm i\omega_p)$. As a consequence, in the second member, terms of frequency equal to ω_p must be avoided. The terms in x_0^2, y_0^2, z_0^2 and $x_0 z_0$ do not raise any problem since they are linearized in $1, \cos(2\omega_p\tau), \sin(2\omega_p\tau)$. The terms $\ddot{x}_0$, $\ddot{y}_0$, $\dot{x}_0$ and $\dot{y}_0$ are linearized in $\cos(\omega_p\tau)$ and $\sin(\omega_p\tau)$ and may generate secular terms. Since ν_1 appears as a multiplicative scalar factor of those terms, it is sufficient to choose $\nu_1 = 0$ to filter out secular terms. With that choice of ν_1, the resulting differential equation is written as

$$\begin{aligned} A^2\ddot{x}_1 - 2A^2\dot{y}_1 - (1 + 2c_2)A^2 x_1 &= \frac{3}{2}(2A_x^2 x_0^2 - A_x^2 y_0^2 - A_z^2 z_0^2), \\ A^2\ddot{y}_1 + 2A^2\dot{x}_1 + (c_2 - 1)A^2 y_1 &= -3c_3 A_x^2 x_0 y_0, \end{aligned}$$

and can be solved explicitly. We find

$$A^2 \begin{pmatrix} x_1(\tau) \\ y_1(\tau) \\ z_1(\tau) \end{pmatrix} = \begin{pmatrix} a_{21}A_x^2 + a_{22}A_z^2 + (a_{23}A_x^2 - a_{24}A_z^2)\cos(2\omega_p\tau + \phi) \\ (b_{21}A_x^2 - b_{22}A_z^2)\sin(2\omega_p\tau + \phi) \\ \delta_r d_{21} A_x A_z (\cos(2\frac{\omega_p}{2}\tau + \psi) - 3) \end{pmatrix},$$

where $\delta_r = 2 - r$, r specifying the class of the orbit, especially its sense of rotation ($r = 1$ for a first class orbit and $r = 3$ for a second class orbit).

Then, the next step consists in plugging the obtained expressions of x_1, y_1 into the equations in the plane (x, y) at the third order, and to choose the parameter ν_2 so as to filter out the possible secular terms. Easy calculations show that one must choose

$$\nu_2 = s_1 A_x^2 + s_2 A_z^2,$$

where

$$\begin{aligned} s_1 &= \frac{\frac{3}{2}c_3(2a_{21}(\kappa^2 - 2) - a_{23}(\kappa^2 + 2) - 2\kappa b_{21}) - \frac{3}{8}(3\kappa^4 - 8\kappa^2 + 8)}{2\lambda(\lambda(1 + \kappa^2) - 2\kappa)}, \\ s_2 &= \frac{\frac{3}{2}c_3(2a_{22}(\kappa^2 - 2) - a_{24}(\kappa^2 + 2) + 2\kappa b_{22} + 5d_{21}) + \frac{3}{8}c_4(12 - \kappa^2)}{2\lambda(\lambda(1 + \kappa^2) - 2\kappa)}, \end{aligned}$$

where $\kappa = \frac{1}{2\lambda}(\lambda^2 + 1 + 2c_2)$, and λ is solution of

$$\lambda^4 + (c_2 - 2)\lambda^2 - (c_2 - 1)(1 + 2c_2) = 0.$$

The expressions of the coefficients a_{ij}, b_{ij} and d_{ij} are given by

$$
\begin{aligned}
a_{21} &= \frac{3c_3(\kappa^2-2)}{4(1+2c_2)}, \quad a_{22} = \frac{3c_3}{4(1+2c_2)},\\
a_{23} &= -\frac{3c_3\lambda}{4\kappa d_1}[3\kappa^3\lambda - 6\kappa(\kappa-\lambda)+4], \quad a_{24} = -\frac{3c_3\lambda}{4\kappa d_1}(2+3\kappa\lambda)\\
a_{31} &= -\frac{9\lambda}{4d_2}(4c_3(\kappa a_{23}-b_{21})+\kappa c_4(4+\kappa^2))\\
&\quad + \left(\frac{9\lambda^2+1-c_2}{2d_2}\right)\left(3c_3(2a_{23}-\kappa b_{21})+c_4(2+3\kappa^2)\right),\\
a_{32} &= -\frac{1}{d^2}\Bigg(\frac{9\lambda}{4}\left(4c_3(\kappa a_{24}-b_{22})+\kappa c_4\right)\\
&\qquad + \frac{3}{2}(9\lambda^2+1-c_2)\left(c_3(\kappa b_{22}+d_{21}-2a_{24})-c_4\right)\Bigg),\\
b_{21} &= -\frac{3c_3\lambda}{2d_1}(3\kappa\lambda-4), \quad b_{22} = \frac{3c_3\lambda}{d_1},\\
b_{31} &= \frac{3}{8d_2}\Bigg(8\lambda\left(3c_3(\kappa b_{21}-2a_{23})-c_4(2+3\kappa^2)\right)\\
&\qquad + (9\lambda^2+1+2c_2)\left(4c_3(\kappa a_{23}-b_{21})+\kappa c_4(4+\kappa^2)\right)\Bigg),\\
b_{32} &= \frac{1}{d_2}\Bigg(9\lambda\left(3c_3(\kappa b_{22}+d_{21}-2a_{24})-c_4\right)\\
&\qquad + \frac{3}{8}(9\lambda^2+1+2c_2)\left(4c_3(\kappa a_{24}-b_{22})+\kappa c_4\right)\Bigg)\\
d_{21} &= -\frac{c_3}{2\lambda^2}, \quad d_{31} = \frac{3}{64\lambda^2}(4c_3a_{24}+c_4),\\
d_{32} &= \frac{3}{64\lambda^2}\left(4c_3a_{23}-d_{21}+c_4(4+\kappa^2)\right),
\end{aligned}
$$

with $d_1 = \frac{3\lambda^2}{\kappa}\left(\kappa(6\lambda^2-1)-2\lambda\right)$ and $d_2 = \frac{8\lambda^2}{\kappa}\left(\kappa(11\lambda^2-1)-2\lambda\right)$.

Secular terms appearing in the third-order z equation cannot be removed by prescribing a coefficient ν_i as previously. It is necessary to specify amplitude and phase angle constraint relationships in order to filter out these secular terms. The amplitude constraint relationship is

$$l_1 A_x^2 + l_2 A_z^2 + \Delta = 0,$$

where $l_1 = a_1 + 2l^2 s_1$ and $l_2 = a_2 + 2l^2 s_2$, with $a_1 = -\frac{3}{2}c_3(2a_{21}+a_{23}+5d_{21}) - \frac{3}{8}c_4(12-k^2)$ and $a_2 = \frac{3}{2}(a_{24}-2a_{22}) + \frac{9}{8}c_4$, and the phase angle constraint relationship is

$$\psi = \phi + \frac{r\pi}{2}, \quad r = 1, 3.$$

Note that the formulas defining the coefficients l_i, $a_{i,j}$, $b_{i,j}$ and d_{ij} are the same than those obtained by Richardson in [31] to determine a third-order approximation of the halo orbits.

With these relations, calculations lead to

$$A^3\begin{pmatrix} x_2(\tau)\\ y_2(\tau)\\ z_2(\tau)\end{pmatrix} = \begin{pmatrix} (a_{31}A_x^3 - a_{32}A_xA_z^2)\cos(3\omega_p\tau+\phi)\\ (b_{31}A_x^3 - b_{32}A_xA_z^2)\sin(3\omega_p\tau+\phi)\\ \delta_r(d_{32}A_zA_x^2 - d_{31}A_z^3)\cos(3\frac{\omega_p}{2}\tau+\psi)\end{pmatrix}.$$

Finally, we arrive at the following third-order approximation of Eight Lissajous orbits:

$$\begin{aligned}
x &= a_{21}A_x^2 + a_{22}A_z^2 - A_x\cos(\tau_1) + (a_{23}A_x^2 - a_{24}A_z^2)\cos(2\tau_1) \\
&\quad + (a_{31}A_x^3 - a_{32}A_xA_z^2)\cos(3\tau_1), \\
y &= kA_x\sin(\tau_1) + (b_{21}A_x^2 - b_{22}A_z^2)\sin(2\tau_1) + (b_{31}A_x^3 - b_{32}A_xA_z^2)\sin(3\tau_1), \\
z &= \delta_r A_z\cos(\tau_2) + \delta_n d_{21}A_xA_z(\cos(2\tau_2) - 3) + \delta_n(d_{32}A_zA_x^2 - d_{31}A_z^3)\cos(3\tau_2),
\end{aligned}$$

where $\tau_1 = \omega_p\tau + \phi$ and $\tau_2 = \frac{\omega_p}{2}\tau + \psi$.

2.3 Computation of a family of Eight Lissajous orbits

In the previous section, a third-order approximation of Eight Lissajous periodic orbits has been calculated analytically. In this section we show how to compute a family of Eight Lissajous orbits, parametrized by the z-excursion A_z. The previous third-order approximation of those orbits, used as an initial guess in a Newton-like procedure, permits to compute some Eight Lissajous orbits but is not precise enough to compute numerically a whole family. One may then try to derive an approximation of greater order, so as to generate a more precise initial guess, in the hope that it will suffice to make converge the Newton procedure. Instead of that, we use here a continuation method on the parameter A_z, in order to generate a family of Eight Lissajous orbits. The procedure is detailed next.

Let us first recall how Newton's method is usually implemented to compute periodic orbits in the restricted three body problem. First, notice that, if $(x(t), y(t), z(t))$ is a solution of the system, then $(x(-t), -y(-t), z(-t))$ is also solution. Given this symmetry, Newton's method consists in determining an adapted initial condition X_0 on the plane $y = 0$, with a velocity orthogonal to this plane,

$$X_0 = (x_0, 0, z_0, 0, \dot{y}_0, 0)^T,$$

generating a semiorbit which reintersects the plane $y = 0$ orthogonally. Fixing the z-excursion z_0, Newton's method consists in adjusting the values of the initial coordinates x_0, $\dot{y}_0$ and the orbital period T so that the corresponding solution verifies $y(\frac{T}{2}) = \dot{x}(\frac{T}{2}) = \dot{z}(\frac{T}{2}) = 0$. This method is first used to compute an Eight Lissajous orbit which serves as an initial point in the continuation method. This shooting method permits to reach a very good precision. Using *Matlab*, we determine x_0, $\dot{y}_0$ and T such that $\|y(\frac{T}{2})\| \leq 10^{-14}$, $\|\dot{x}(\frac{T}{2})\| \leq 10^{-14}$ and $\|\dot{z}(\frac{T}{2})\| \leq 10^{-14}$. Newton's method is then used at every step of the iteration procedure of the continuation method described next.

Let A_z be the z-excursion of the Eight Lissajous orbit to be computed, and X_0 the corresponding initial condition to be determined. If A_z^0 is the z-excursion of the first Eight Lissajous orbit computed thanks to the third-order approximation, the continuation method consists in making the z-excursion vary from A_z^0 to A_z, according to an appropriate subdivision, and solving at each iteration the Newton's problem initialized with an initial condition which is the final point obtained from the previous step.

More precisely, let A_z^n be the n-th z-excursion of the subdivision. Assume that each Eight Lissajous orbit has already been computed for A_z^p, $p \in 1, \ldots, n$, the resulting initial condition being noted X_0^p. In order to compute the Eight Lissajous orbit of z-excursion A_z^{n+1}, the continuation method consists in using the initial condition X_0^n as a first guess for the Newton's method. If the subdivision is fine enough chosen, then

the Newton's method converges to a point which is then chosen as initial guess X_0^{n+1}. The latter is used to compute the Eight Lissajous orbit of z-excursion A_z^{n+1}, and the procedure goes on by iteration, until the Eight Lissajous orbit of z-excursion A_z is computed. Table (1) summarizes the continuation procedure.

Initial information	Newton's method	Numerical results
A_z^0, X_0^0	$\longrightarrow$	X_0^1
	$\swarrow$	
A_z^1, X_0^1	$\longrightarrow$	X_0^2
	$\swarrow$	
$\vdots$	$\vdots$	$\vdots$
	$\swarrow$	
A_z^{n-1}, X_0^{n-1}	$\longrightarrow$	X_0^n
	$\swarrow$	
A_z, X_0^n	$\longrightarrow$	X_0

Table 1 Continuation method algorithm

A single Eight Lissajous orbit around Lunar L_1 (that is the Lagrange point L_1 in the Earth-Moon system) is represented on Figure (4) in position and velocity spaces.

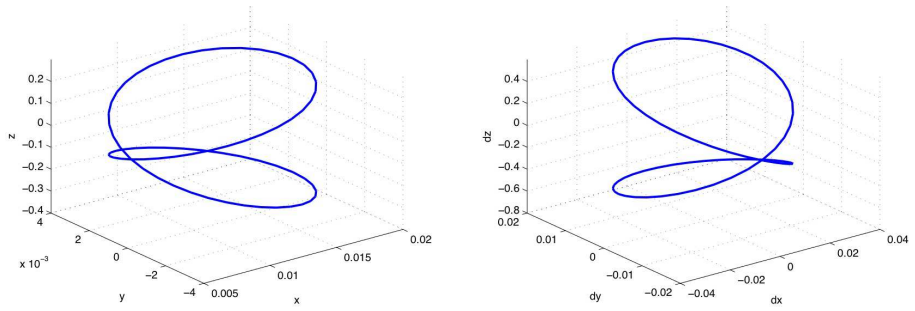

(a) (b)

Fig. 4 (a) Eight Lissajous orbit around Lunar L_1 in the position space. (b) Eight Lissajous orbit around Lunar L_1 in the velocity space.

Figure 5 represents the projections of a family of Eight Lissajous orbits on the planes (x, y), (y, z) and (x, z) computed using the continuation method.

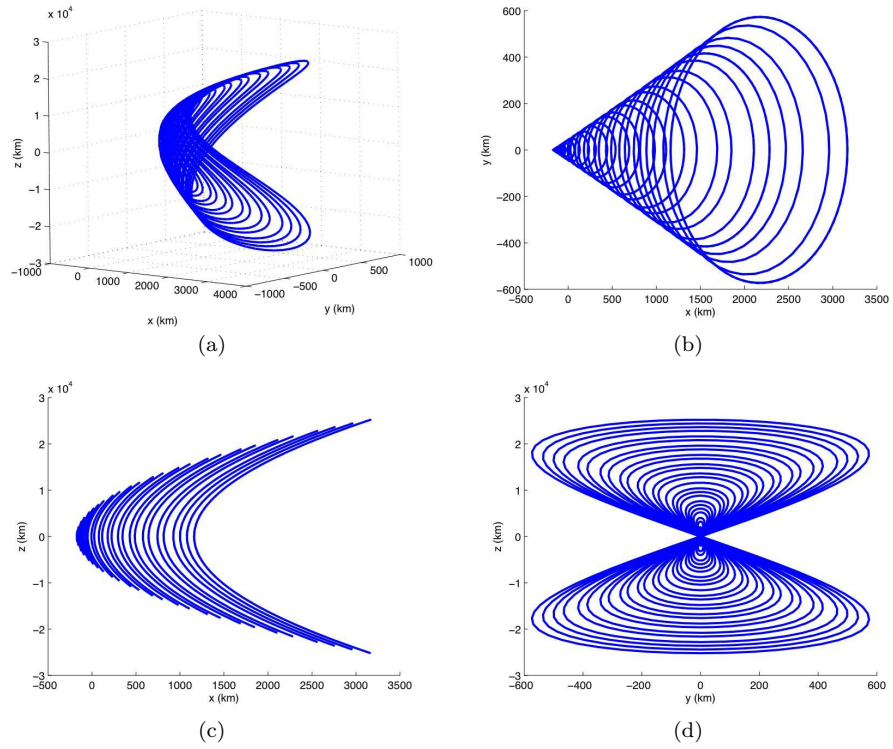

Fig. 5 Family of Eight Lissajous orbits and their projection on the (x, y), (y, z) and (x, z)-planes.

3 Properties of invariant manifolds of Eight Lissajous orbits

3.1 Empiric stability

The interest of Eight Lissajous orbits is essentially based on two properties presented by their invariant manifolds. The stable (resp., unstable) manifold of an Eight Lissajous orbit is the submanifold of the phase space which is formed by all points whose future (resp., past) semi-orbits converge to it (asymptotic orbits). Locally, in the neighborhood of the Eight Lissajous orbit, they look like eight-shaped tubes (see Figure 6).

To compute the invariant manifolds, their linear approximation is first used around periodic orbits. At each point a of a given Eight Lissajous orbit Σ, one computes the eigenvectors $V^s(a)$ and $V^u(a)$ associated to the real eigenvalues of the monodromy matrix at a that are lower and greater than 1. Then, one gets an approximation of the stable and unstable manifolds by propagating the orbits solutions of the equations of motion starting from initial conditions

$$X_0 = a + \epsilon V(a),$$

where a belongs to the Eight Lissajous orbit, $V(a)$ is a normalized stable or unstable eigenvector of the monodromy matrix at a, and ϵ is a real, small enough so as to

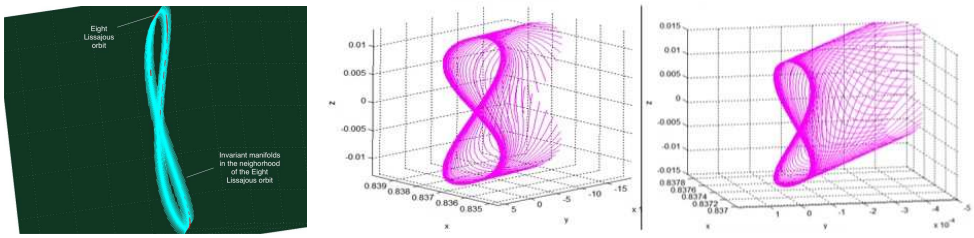

Fig. 6 Invariant manifolds in the neighborhood of an Eight Lissajous orbit

ensure a good linear approximation is correct but also not too small in order to avoid too long integration times. Indeed, the asymptotic orbits which form the invariant manifolds rotate strongly when tending to the Eight Lissajous orbit (see e.g. [19]). Some numerical results are provided on Figure 7, for the Lagrange point L_1 in the Earth-Moon system.

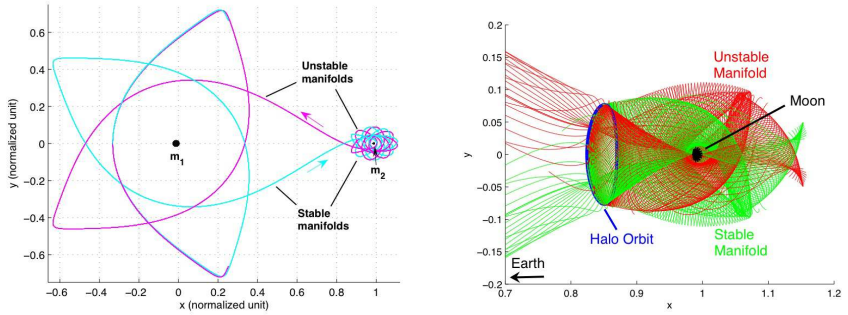

(a) Invariant manifolds of an Eight Lissajous orbit

(b) Invariant manifolds of a halo orbit

Fig. 7 Invariant manifolds of an Eight Lissajous orbit and of a halo orbit

A first important property that we observe on the numerical simulations is that the invariant manifolds of Eight Lissajous orbits seem to keep the same structure in large time. This global stability property which is numerically observed is also illustrated on Figure 8 where different images by the flow of an Eight Lissajous orbit at different times are represented.

This property is of particular interest for mission design. Note that such a stability property does not hold for halo orbits. Indeed, the invariant manifold of a classical halo orbit have the aspect of a regular tube in the neighborhood of the orbit but this regular aspect is not persistent far away from the halo orbit and/or in large integration time; in particular these tubes behave in a chaotic way in large time (see Figure 7). In contrast, the regular structure of invariant manifolds of Eight Lissajous orbits is conserved even after a large integration time. This global stability property may be relevant for mission computation since it allows to predict the behavior of the trajectories which propagate on and inside these invariant manifolds in large time. We next investigate in more

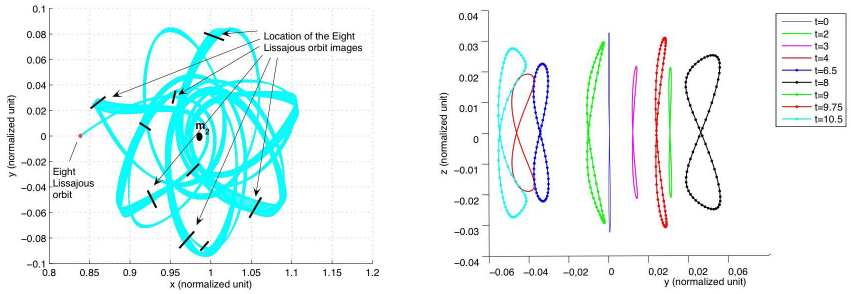

(a) Invariant manifold of an Eight Lissajous orbit around the Lagrange point L_1 in the Earth-Moon system

(b) Images by the flow of the Eight Lissajous orbit at different times

Fig. 8

details these stability properties of invariant manifolds of halo and Eight Lissajous orbits using Lyapunov exponents.

3.2 Local Lyapunov Exponents

The concept of Lyapunov exponents, introduced in [23], is used here to investigate stability properties of invariant manifolds of Eight Lissajous orbits. Lyapunov exponents measure the exponential convergence or divergence of nearby trajectories in a dynamical system. They provide indications on the behavior in large time of solutions under infinitesimal perturbations. A positive Lyapunov exponent means that nearby trajectories may diverge, whereas a negative Lyapunov exponent indicates a stability property. In [1], the authors define and compute local Lyapunov exponents in several types of motion using a result of Osedelec (see [29]). In [35], algorithms are presented, which permit to estimate Lyapunov exponents from an experimental time series. In [2], a stability technique based on local Lyapunov exponents is applied for maneuver design and navigation in the three-body problem. Finally, it is shown in [8] that finite-time Lyapunov exponents can provide useful information on the qualitative behavior of trajectories in the context of astrodynamics. Local Lyapunov exponents are used to determine the behavior of nearby trajectories in finite time. They provide indications on the effects that perturbations or maneuvers will have on trajectories after a specified duration. In the case of the circular restricted three-body problem, which is known to be chaotic, local Lyapunov exponents cannot be expected to be negative. It is however interesting to use local Lyapunov exponents in our study to measure the stability of Eight Lissajous orbits and of their invariant manifolds, and compare it with the stability of classical halo orbits and of their invariant manifolds.

Let us first recall the way to compute such Lyapunov exponents. Let $\dot{x} = f(x,t)$ stand for the equations of motion, and let $x(\cdot)$ be a reference trajectory, supposed to be defined on $[0,+\infty)$. Let $t \geq 0$. Consider a perturbation term $\delta x(t)$; the solution of the linearized equation along $x(\cdot)$, starting from t, is given by

$$\delta x(\cdot) = \Phi(\cdot,t)\delta x(t)$$

where $\Phi(\cdot, t)$ is the state transition matrix. For $\Delta > 0$, the local Lyapunov exponent (in short, LLE) $\lambda(t, \Delta)$ is defined by

$$\lambda(t, \Delta) = \frac{1}{\Delta} \ln \left(\text{maximal eigenvalue of } \sqrt{\Phi(t+\Delta, t)\Phi^T(t+\Delta, t)} \right). \tag{9}$$

Note that, if Δ tends to $+\infty$, one recovers the usual Lyapunov exponent. The parameter Δ stands for a positive duration over which the effect of perturbations is tested. In other words, the LLE $\lambda(t, \Delta)$ provides an indication on the effect a perturbation at time t would be expected to have over a duration Δ.

When Δ is large, the eigenvectors of the matrix $\sqrt{\Phi(t+\Delta, t)\Phi^T(t+\Delta, t)}$ tend to align along the eigenspace associated with the maximal eigenvalue. A Gram Schmidt reduction procedure may be used for the computation of Lyapunov exponents so as to identify the eigenelements. Nevertheless, since we are only interested in the maximal eigenvalue of $\sqrt{\Phi(t+\Delta, t)\Phi^T(t+\Delta, t)}$, this procedure is not necessary. Concerning the units, the Lyapunov exponents measure the rate at which a system creates or destroys information, and are usually expressed in information/s.

In our study, the local Lyapunov exponents were computed every 0.1-day time step along selected trajectories, with $\Delta = 1$ day (see Figure 9). Note that similar results are obtained for other values of Δ (for instance, $\Delta = 20$ days), and thus are not reported here.

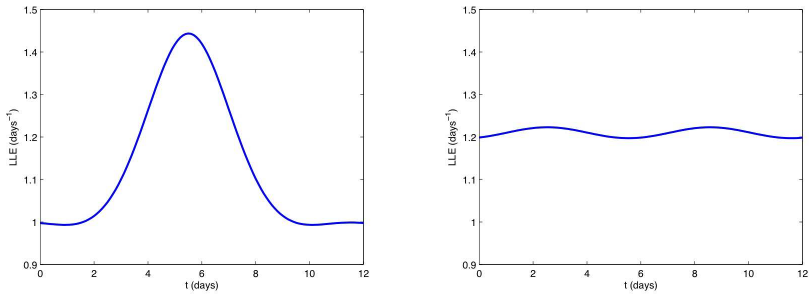

(a) (b)

Fig. 9 (a) Local Lyapunov exponent of a halo orbit. (b) Local Lyapunov exponent of a Eight Lissajous orbit.

On Figure (9), LLE are computed along a halo orbit and an Eight Lissajous orbit of similar energy, around the Lagrange point L_1 in the Earth-Moon system. The first observation that can be done is that in both cases, the LLE are positive. As said before, this is due to the chaotic character of the whole system. This means that in both cases, nearby trajectories of the periodic orbit may diverge over a certain time period. However both LLE behave differently. On the one hand, the maximal value of the LLE of the halo orbit is greater than the values of the LLE of the Eight Lissajous orbit, which remains almost constant. On the other hand, the interval between minimal and maximal values of the LLE of the halo orbit contains the set of values of the LLE of the Eight Lissajous orbit, and the mean values of the LLE of both orbits seem to be almost the same. This fact can be explained from the following fact: the closer

a trajectory gets from a primary (the Moon in this case), the higher its LLE will be. Since the Eight Lissajous orbit is almost vertical, its distance from the primaries remains almost the same during all its period, and its LLE remains almost constant too. On the contrary, for the same value of energy, the x-excursion of the halo orbit varies a lot (several thousands of kilometers) and hence the orbit gets closer to the Moon. Its LLE varies from a minimal value corresponding to the furthermost point to the Moon, to a maximal value corresponding to the closest point to the Moon. Depending on the energy value, this maximal value gets larger as the orbit gets closer to the Moon. Finally, the stability properties of these periodic orbits are related to their the geographic situation. Their specificities make that the plots of their LLE versus time are different, but their geographic situation around the same Lagrange point makes that none of them can be said more stable than the other.

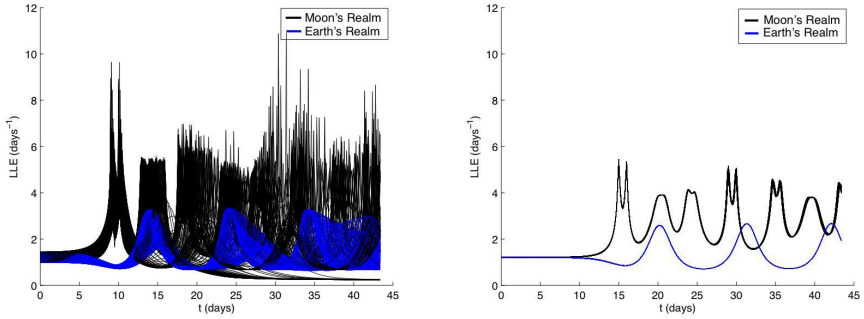

(a) (b)

Fig. 10 (a) Local Lyapunov exponent of the invariant manifolds of a halo orbit. (b) Local Lyapunov exponents of the invariant manifolds of a Eight Lissajous orbit.

The situation is completely different for their invariant manifolds. On Figure (10), local Lyapunov exponents are computed along the invariant manifolds of the previous halo and Eight Lissajous orbits. The stability difference was not evident concerning the periodic orbits, but this is not the case for their invariant manifolds. In the Earth's realm (in blue on the figure), the LLE of the invariant manifolds are close for both periodic orbits (by looking closer, the LLE of the Eight Lissajous orbit manifolds is shown to be lower but the difference is small). In the Moon's realm, the stability difference is evident. The LLE of the halo orbit manifolds reach 11 days$^{(-1)}$ whereas the LLE of the Eight Lissajous manifolds keeps values lower than 5 days$^{(-1)}$ and the difference is similar concerning the mean values. It confirms that some trajectories of the halo orbit manifolds (and the manifolds themselves) are very unstable. As a consequence, predicting the behavior of such a trajectory may happen to be difficult. Things are going differently for the asymptotic trajectories forming the Eight Lissajous manifolds. Their LLE indicate possible instabilities but, in spite of their small distance to the Moon (which, as mentioned previously, may create instabilities), their LLE keep reasonable values. Notice also that the plot of the LLE of the Eight Lissajous manifolds has a very smooth aspect, in contrast with the chaotic aspect of the LLE of halo orbit manifolds. This is in accordance with the fact that the Eight Lissajous manifolds keep

their regular structure of eight-shaped tube even after a large integration time. This nice stability property in large time of the Eight Lissajous manifolds is of potential interest for mission design with low cost.

3.3 Accessible lunar region with the Eight Lissajous invariant manifolds in the Earth-Moon system

The second interesting property concerning the invariant manifolds of Eight Lissajous orbits is based on the large accessible lunar region that they cover in large time. By propagating the invariant manifolds of an Eight Lissajous orbit, we observe an oscillating behavior around both primaries. The invariant manifolds which oscillate around the bigger primary stay rather far from it but the invariant manifolds around the smaller one get close to it. Our application concerns the Earth-Moon system, and we observe that the invariant manifolds of the Earth region stay too far from the Earth to plan a mission using them for a direct departure from the Earth, but the invariant manifolds which oscillate around the smaller primary (the Moon) oscillate close to it and thus may be used for a departure or a capture around the Moon (see Figure 11).

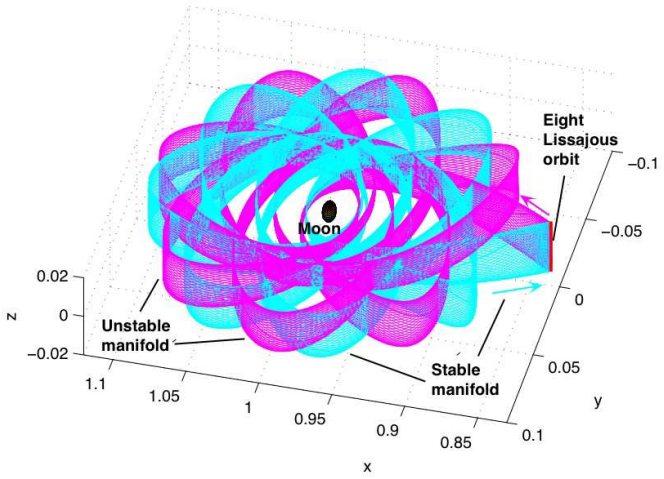

Fig. 11 Invariant manifolds of an Eight Lissajous orbit in the neighborhood of the Moon.

The oscillation of these invariant manifolds is not new compared with what can be observed in the classical case of halo orbits. Nevertheless, the constant oscillation of invariant manifolds of Eight Lissajous orbits in the lunar region on the one part, and global eight-shaped structure of these manifolds on the other part, are interesting properties for mission design. Indeed, such invariant manifolds may be used to visit almost all the surface of the Moon, at any time, as shown next.

Lunar strip covered by the invariant manifolds. On Figure 12, we have computed the projection on the Moon of invariant manifolds of an Eight Lissajous orbit. We observe

that, over a long period, a large surface of the Moon may be scanned, depending on the value of the z-excursion of the orbit.

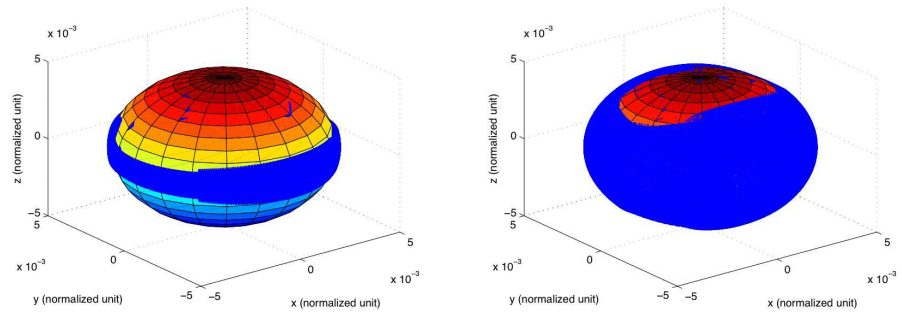

(a) (b)

Fig. 12 Lunar strip covered by the invariant manifolds for (a) Az=10000 km and (b) Az=50000 km.

First, on Figure 12, we observe that, for every value of the z-excursion of the Eight Lissajous orbit, every longitude can be reached. This is due to the oscillation property observed previously. However, this oscillation staying at the equator's level, the latitudes flied over by the manifolds depend on the z-excursion of the Eight Lissajous orbit. If the z-excursion is small, then the latitudes reached are small too. Larger latitudes are reached whenever the z excursion is getting larger. For a z-excursion value equal to 50000 km, and for larger values of the z-excursion, almost all the lunar surface can be scanned from the invariant manifolds. Only the poles cannot be reached directly. A maneuver should be performed to fly over the lunar poles. Anyway, these results show the relevance of invariant manifolds of Eight Lissajous orbits to scan almost all the Moon's surface at low cost.

The perigee-angle representation. To complete the previous results, we provide the plot of the invariant manifolds in the perigee-angle plane. For each asymptotic trajectory of the invariant manifolds, the minimal distance to the Moon (perigee) and the corresponding latitude (angle) are computed.

On Figure 13, it is observed that the angles of the perigees range between 20 and 45 degrees. The fact that the range of angles drawn on this figure is smaller than the range of angles covered by the manifolds is not contradictory, since trajectories of invariant manifolds, close to the Moon, reach their closest point to the Moon for a value of inclination between 20 to 45 degrees. Notice that these closest points correspond to positions on the hidden face of the Moon and generally occur at the first oscillation of the manifold around the Moon, i.e, in short time.

Figure 13 shows that the minimal distance to the Moon oscillates between 1500 and 5000 kilometers, depending on the z-excursion of the Eight Lissajous orbit (see Table 2). The minimal distances are reached after a 9-to-50 days journey from the periodic orbit, but it is clear that for each trajectory 9 days are sufficient to get close enough to the Moon to be captured.

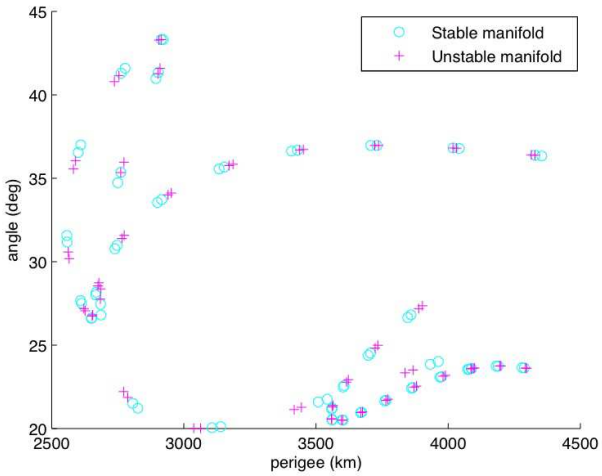

Fig. 13 Invariant manifolds of Eight Lissajous orbits in the perigee-angle plane

The results about the invariant manifolds oscillating around the Earth are not provided here, since they do not appear to be as relevant as those concerning the Moon. We however mention that the minimal distance between the manifolds of the exterior realm and the Earth oscillate between 115000 and 125000 km, also depending on the value of the z-excursion, with a 40-days journey between the perigee and the Eight Lissajous orbit. This journey duration can be half reduced since similar approach distances are reached after 20 days. In both cases, the corresponding inclinations are meaningless given the large distance between the manifolds and the Earth. One can just observe that the invariant manifolds oscillate around the Earth at the equator level.

Finally, these results highlight the potential interest of Eight Lissajous orbits and of their invariant manifolds. Using them, every point located on a band encircling the lunar equator may be reached from the periodic orbit. Except the poles, almost every point of the lunar surface may be flied over from an Eight Lissajous orbit with a large z-excursion. Note that this may be realized at any time since the ephemeride is not considered in the restricted three-body problem.

z-excursion of the Eight Lissajous orbit (in km)	Approach time to the Earth (in days)	Approach distance to the Earth (in km)	Approach time to the Moon (in days)	Approach distance to the Moon (in km)
1000	40	116730	43	1673
5000	40	116650	43	1627
10000	40	116800	43	1514
20000	40	117380	9	4502
30000	40	118340	9	5122
40000	40	119670	39	3280
50000	40	121340	42	3333

Table 2 Minimal approach time and distance of the manifolds to the Earth and to the Moon in function of the z-excursion of the Eight Lissajous orbit.

Conclusion

In this article, we focused on particular periodic orbits around Lagrange points in the circular restricted three-body problem, called Eight Lissajous orbits. A third-order approximation of these orbits has been established using Lindstedt-Poincaré's method. Families of Eight Lissajous orbits have been computed using a shooting method combined with a continuation method, the previous third-order approximation serving as an initial guess. Then, we have shown that Eight Lissajous orbits have interesting features. First, their invariant manifolds keep in large time a stable eight-shaped structure, in contrast to those of halo orbits. This fact has been put in evidence by computing local Lyapunov exponents. Second, in the Earth-Moon system, we have shown that invariant manifolds of Eight Lissajous orbits permit to scan almost all the Moon surface, depending on the value of the z-excursion. These properties are of potential interest for mission design at low cost. Of course such strategies may require a long time transfer and then a compromise has to be found between the energy consumption and the time of transfer. Note also that, having in mind an Earth-Moon mission, invariant manifolds oscillating around the Earth cannot be used directly for a departure from the Earth, due to their too large distance. At the contrary, the stability of the Eight Lissajous orbits invariant manifolds and the accessibility to the lunar surface provide interesting perspectives, such as easy and economic communications between a spacecraft exploring the Moon and an orbital station based on an Eight Lissajous orbit around the Lagrange points $L1$ or $L2$ in the Earth-Moon system. From such an orbital station, almost every point of the Moon may be visited at any time with a low cost.

References

1. Abarbanel, H.D.I., R. Brown, and M.B. Kennel. Variation of Lyapunov Exponents on a Strange Attractor, *Journal of Nonlinear Science, Vol.1, 1991, pp. 175-199*.
2. Rodney L. Anderson, Martin W. Lo and George H. Born (2003). Application of Local Lyapunov Exponents to Maneuver Design and Navigation in the Three-Body Problem. *AAS 03-569*.
3. Belbruno Edward A. and Carrico John P. (2000). Calculation of Weak Stability Boundary Ballistic Lunar Transfer Trajectories. *AIAA 2000-4142*.
4. Benettin Giancarlo, Galgani Luigi, Giorgilli Antonio and Strelcyn Jean-Marie (1980). Lyapunov Characteristic exponents for smooth dynamical systems and for hamiltonian systems; a method for computing all of them. Part 1: Theory, and Part 2: Numerical Application. *Meccanica*, March 1980.
5. Benettin Giancarlo, Galgani Luigi and Strelcyn Jean-Marie (1976). Kolmogorov entropy and numerical experiments. *Physical Review A, Vol. 14, Num. 6, 1976*.
6. Bonnard B., Faubourg L. and Trélat E. (2005). Mécanique céleste et contrôle des véhicules spatiaux. *Mathématiques et Applications 51*.
7. Breakwell John V. and Brown John V. (1979). The halo family of 3-dimensional of periodic orbits in the Earth-Moon restricted 3-body problem. *Celestial Mechanics 20, pp. 389-404, 1979*.
8. Dellnitz M., Padberg K. , Post M., and Thiere B. (2007). Set Oriented Approximation of Invariant Manifolds: Review of Concepts for Astrodynamical Problems. *New trends in astrodynamics and applications III*, AIP Conference Proceedings, Vol. 886, pp. 90-99 (2007).
9. Dunham David W. and Farquhar Robert W. (1978-2002). Libration Points Missions. *International Conference on Libration Points and Applications* (Girona, Spain, 10-14 June, 2002).
10. Euler L. (1767). De motu rectilineo trium corporum se mutuo attrahentium. *Novi commentttarii academiae scientarum Petropolitanae*, **11**, 144–151. In Oeuvres, Seria Secunda tome XXv Commentationes Astronomicae (page 286).

11. Farquhar Robert W. (1966). Station-keeping in the vicinity of collinear libration points with an application to a Lunar communications problem. Space Flight Mechanics, Science and Technology Series **11**, 519–535.
12. Farquhar Robert W. (1972). A Halo-Orbit Lunar Station. *Astronautics & Aeronautics*, Vol. 10, No. 6, 59-63, 1972.
13. Gómez, G., W. S. Koon, M. Lo, J. E. Marsden, J. Masdemont, and S. D. Ross (2001). Invariant manifolds, the spatial three-body problem and space mission design. Adv. Astronaut. Sci. **109**, 3–22.
14. Gómez, G., W. S. Koon, M. Lo, J. E. Marsden, J. Masdemont, and S. D. Ross (2004). Connecting orbits and invariant manifolds in the spatial three-body problem, *Nonlinearity*, **17**, 1571-1606.
15. G. Gómez, J. Masdemont, and C. Simó (1997). Lissajous orbits around halo orbits. Adv. Astronaut. Sci. **95**, 117–34.
16. G. Gómez, J. Masdemont, and C. Simó (1998). Quasihalo orbits associated with libration points. J. Astronaut. Sci. **46**, 135–76.
17. K.C. Howell, H.J. Pernicka (1988). Numerical determination of Lissajous orbits in the restricted three-body problem. Celestial Mechanics **41**, 107–124.
18. A. Jorba, J. Masdemont (1999). Dynamics in the center manifold of the collinear points of the restricted three-body problem. Physica D **132**, 189–213.
19. Koon W. S., Lo M. W., Marsden J. E., Ross S. D. (2005). Dynamical systems, the Three-Body Problem and Space Mission Design.
20. Lagrange, J.-L. (1772). Essai sur le problème des trois corps, 1772. Prix de l'académie royale des Sciences de paris, tome IX, in vol. 6 of *Oeuvres de Lagrange* (Gauthier-Villars, Paris, 1873), 272–282.
21. Lo, M. W. and Ross, S. D.(1998). The Lunar L1 Gateway: Portal to the Stars and Beyond. *AIAA Space 2001 Conference* (Albuquerque, New Mexico, August 28-30), 2001.
22. Lo, M. W. and Chung, M. J.(2002). Lunar Samplar Return via the Interplanetary Highway. *Paper AIAA 2002-4718, AIAA/AAS Astrodynamics Specialist Conference and Exhibit* (Monterey, California, August 5-8), 2002.
23. Lyapunov A. M. The General Problem of the Stability of Motion. *Comm. Soc. Math. Kharkow (in Russian, reprinted in English, Taylor & Francis, London, 1992)*, 1892.
24. Marsden J. E., Koon W. S., Lo M. W., Ross S. D. (2001). Low energy transfer to the Moon, *Celestial Mechanics Dyn. Astron.*, **81**, 27-38.
25. McLaughlin W. I. (2000). Walter Hohmann's roads in space, *Journal of Space Mission Architecture*, (2000).
26. Meyer, K. R., Hall, G.R. (1992). Introduction to Hamiltonian dynamical systems and the N-body problem, *Applied Mathematical Sciences 90*, Springer-Verlag, New-York (1992).
27. Miller J.K. and Belbruno E.A. (1993). Sun-Perturbated Earth-to-Moon Transfers with Ballistic Capture. *Journal of Guidance, Control and Dynamics*, Vol. 16, No. 4, 770-775 (1993).
28. Moser J. (1958). On the generalization of a theorem of A. Lyapunov. Commun. Pure Appl. Math. **11**, 257–271.
29. Osedelec, V.I., A Multiplicative Ergodic Theorem Lyapunov Characteristic Numbers for Dynamical Systems, *Trudy Moskov. Mat. Obsc. 19, Transaction of the Moscow Mathematical Society*, Vol. 19, 1968, pp. 197-231.
30. Poincaré H. (1893). New methods of Celestial Mechanics, *American Institute of Physics.*
31. Richardson D.L. (1980). Analytic Construction of periodic orbits about the collinear points, *Celestial mechanics 22*, 241–253.
32. Ross, S. D., W. S. Koon, M. W. Lo, and J. E. Marsden (2004). Design of dynamical systems theory to a very low energy transfer, in the *14th AAS/AIAA Space Flight Mechanics Meeting*, Maui, Hawaii, Paper No. AAS 04-289.
33. Ross S.D. Cylindrical Manifolds and Tubes Dynamics in the Restricted Three-Body Problem (Ross Thesis), California Institute of Technnology, Pasadena, California (2004).
34. Szebehely, V. G. (1967). Theory of orbits : the restricted problem of three bodies, *Academic Press*, New-York (1967).
35. Wolf Alan, Jack B. Swift, Harry L. Swinney and John A. Vastano (1985). Determining Lyapunov exponents from a time series. *Physica*, North-Holland, Amsterdam (1985).
36. Zazzera F., Bernelli, F. Topputo, and Massari M. (2004). Assessment of mission design including utilization of libration points and weak stability boundaries.